View metadata, citation and similar papers at core.ac.uk

brought to you by CORE

provided by IUPUIScholarWorks

ACCEPTED MANUSCRIPT

Fracture behavior and thermal durability of lanthanum zirconate-based thermal barrier coatings with buffer layer in thermally graded mechanical fatigue environments

Guanlin Lyu[1], Bong Gu Kim[1], SeoungSoo Lee[1], Yeon-Gil Jung[*,1],

Jing Zhang[2], *Baig-Gyu Choi*[3], In-Soo Kim[3]

[1]School of Materials Science and Engineering, Changwon National University,

Changwon, Gyeongnam 641-773, Republic of Korea

[2]Department of Mechanical Engineering, Indiana University-Purdue University Indianapolis,

Indianapolis, IN 46202, USA

[3]High Temperature Materials Research Group, Korea Institute of Materials Science,

Changwon,Gyeongnam 51508, Korea

[*]Corresponding author: Prof. Yeon-Gil Jung

Tel: +82-55-213-3712/ Fax: +82-55-262-6486

E-mail: jungyg@changwon.ac.kr

This is the author's manuscript of the article published in final edited form as:

Lyu, G., Kim, B. G., Lee, S., Jung, Y.-G., Zhang, J., Choi, B.-G., & Kim, I.-S. (2017). Fracture behavior and thermal durability of lanthanum zirconate-based thermal barrier coatings with buffer layer in thermally graded mechanical fatigue environments. Surface and Coatings Technology. https://doi.org/10.1016/j.surfcoat.2017.09.066

ACCEPTED MANUSCRIPT

Abstract

The effects of buffer layer on the fracture behavior and lifetime performance of lanthanum zirconate ($La_2Zr_2O_7$; LZO)-based thermal barrier coatings (TBCs) were investigated through thermally graded mechanical fatigue (TGMF) tests, which are designed to simulate the operating conditions of rotating parts in gas turbines. To improve the thermal durability of LZO-based TBCs, composite coats consisting of two feedstock powders of LZO and 8 wt.% yttria-doped stabilized zirconia (8YSZ) were prepared by mixing different volume ratios (50:50 and 25:75, respectively). The composite coat of 50:50 volume ratio was employed as the topcoat, and two types of buffer layers were introduced (25:75 volume ratio in LZO and 8YSZ, and 8YSZ only). These TBC systems were compared with a reference TBC system of 8YSZ. The TGMF tests with a tensile load of 60 MPa were performed for 1000 cycles, at a surface temperature of 1100 °C and a dwell time of 10 min, and then the samples were cooled at room temperature for 10 min in each cycle. For the single-layer TBCs, the composite topcoat showed similar results as for the reference TBC system. The triple-layer coating (TLC) showed the best thermal cycle performance among all samples, suggesting that the buffer layer was efficient in improving lifetime performance. Failure modes were different for the TBC systems. Delamination and/or cracks were created at the interface between the bond and topcoats or above the interface in the single-layer TBCs, but the TBCs with the buffer layer were delaminated and/or cracked at the interface between the buffer layer and the topcoat, independent of buffer layer species. This study allows further understanding of the LZO-based TBC failure mechanisms in operating conditions, especially in combined thermal and mechanical environments, in order to design reliable TBC systems.

ACCEPTED MANUSCRIPT

Keywords: Thermal barrier coating; Lanthanum zirconate; Structural design; Thermally graded mechanical fatigue test; Thermal durability

1. Introduction

Thermal barrier coating (TBC) systems have been widely applied in hot section parts of gas turbine engines to provide thermal protection to metallic components from high temperature service environments [1,2]. Obviously, TBCs protect the underlying substrate against the high temperature oxidation and corrosion, enhance the operational life of hot section components, and increase the fuel efficiency of gas turbine engines by improving turbine inlet temperature (TIT). The fracture behavior and thermal durability of TBC systems are usually investigated in either thermal cycling or mechanical loading. Especially, in the case of moving parts such as turbine blades, not only is a thermal gradient generated between the heating and cooling surfaces of a blade, but the centrifugal force also increases due to the rapid rotational speed of 3600 rpm [3]. Thus, the TBC system employed on turbine blades is subjected to both thermal and mechanical stresses, which may easily cause premature failures. Therefore, the lifetime performance of the TBC system, especially in the case of moving parts, should be evaluated in dual environments.

TBC systems usually consist of a superalloy substrate, an oxidation-resistant metallic bond coat, and a ceramic topcoat. The classic topcoat in a TBC system is 7–8 wt.% yttria-stabilized zirconia (ZrO_2, 7–8YSZ) which has a high melting point (2680 °C) *[4]*, relatively low thermal conductivity (2.0–2.3 W/m/K at ~1000 °C for a fully dense sample; 0.9–1.2 W/m/K for 10–15% porosity) *[5–7]*, and favorable thermal stability *[8,9]*. As the TIT is continuously increasing in gas turbines, there is a limitation in application of 8YSZ-

ACCEPTED MANUSCRIPT

coating systems, especially above 1200 °C. YSZ transforms from the t′ phase to the tetragonal and cubic phases (t and c phases, respectively) by repetitive heating and cooling process above 1200 °C, and then to the monoclinic (m) phase with a volume expansion of about 3–5 vol% in further operation, resulting in the spallation or delamination of the coating systems [4,7]. To solve these problems, lanthanum zirconate ($La_2Zr_2O_7$, LZO) has been proposed as a new material for TBC application. Compared to 8YSZ, LZO has a lower conductivity (1.5–1.8) W/m/K at 1000 °C, no phase transition from room temperature to melting point, a lower oxygen ion diffusivity, which protects the bond coat and the substrate from oxidation [4,9], a lower coefficient of thermal expansion (CTE) (9.1×10^{-6}–9.7×10^{-6} K^{-1} for LZO, compared to 10.5×10^{-6}–11.5×10^{-6} K^{-1} for YSZ, bulk materials and coatings at 30–1000 °C), and lower sintering ability *[10]*.

LZO does have shortcomings, such as lower CTEs and mechanical properties than 8YSZ. TBC systems with LZO can be used if the CTE of the LZO is selected to give a TBC system that is similar to a system with an 8YSZ coating, and the mechanical properties of the TBC systems with LZO are improved to be comparable with those of TBC systems with 8YSZ. However, there is no single material that satisfies all requirements for TBCs. Multilayer concepts have been put forward, which include an erosion-resistant layer as an outer layer, a thermal barrier layer, a corrosion–oxidation-resistant layer, a thermal stress control layer, and a diffusion-resistant layer *[11]*. However, multilayered structures can produce artificial defects at the layer interfaces, which can cause delamination or cracking. Therefore, a double-layer top coat *(DLC) system*, based on the multilayer concept, has been shown to be an effective method to meet the demands of developing TBC systems *[10,12]*. The DLC includes a ceramic topcoat layer, a ceramic

ACCEPTED MANUSCRIPT

buffer layer, a bond coat layer, and a superalloy substrate. The buffer layer is introduced between the top and bond coats, which can reduce stresses generated at the interface due to the CTE mismatch between the top and bond coats during cyclic thermal exposure. In addition, in a previous study *[13]*, layered LZO-based TBCs were already investigated through furnace cyclic thermal fatigue, thermal shock, and jet engine thermal shock tests. However, these methods evaluated the thermal durability in the cyclic thermal exposure, but not both thermal and mechanical stress environments.

In this study, LZO-based TBC systems with a layered topcoat structure were designed using blended feedstock of LZO and 8YSZ powders prepared by mixing in different volume ratios. Three types of the layered LZO-based TBCs were tested at room temperature and 1100 °C under a tensile load of 60 MPa to simulate a gas turbine blade subject to centrifugal force and high temperature gas flow, using a thermally graded mechanical fatigue (TGMF) test. The thermal durability and fracture behavior of the layered LZO-based TBCs were investigated and compared with those of the single-layer TBCs. The effects of the buffer layer structure and species at the interface on the lifetime performance of TBCs were also investigated through TGMF tests.

2. Experimental Procedure

2.1. Starting materials and sample preparation

The substrate was an approximately 5.5 mm thick nickel-based superalloy (Hastelloy-X, nominal composition of 47Ni–22Cr–18Fe–9Mo, in wt.%). The dimensions of the sample are shown in Fig. 1(A). The surface was blasted using alumina powder with a particle size of 60 mesh and then cleaned before deposition. The bond coat was prepared

ACCEPTED MANUSCRIPT

by an air-plasma spray (APS) method (9 MB; Sulzer Metco Holding AG, Switzerland) using an AMDRY 962 (hereinafter 962, nominal composition of Ni–22Cr–10Al–1.0Y in wt.% and particle size of 56–106 μm; Sulzer Metco Holding AG). The feedstock for the topcoat was blended with 8YSZ and LZO. These powders were employed as METCO 204C-NS (hereinafter 204C-NS, particle size of 45–125 μm; Sulzer Metco Holding AG) and LAO-109-1 (Praxair Surface Technologies, Indianapolis, USA), respectively. Surface and side photographs of the as-prepared LZO-based TBC sample is shown in Fig. 1(B). The blended powders of 8YSZ and LZO were prepared by mixing 50:50 and 75:25 volume ratios for the topcoat and buffer layers, respectively. Note that the buffer layer was introduced in the LZO-based TBC for reducing thermal mismatch between the bond and topcoats. The thicknesses of the bond coat and topcoat were designed to be 150 μm and 430 μm, respectively. Three kinds of LZO-based TBCs were prepared, including a single-layer top coat (SLC), a DLC, and a triple-layer top coat (TLC) with double buffer layers. The SLC consists of the bond coat and the top coat with 50:50 volume ratio in LZO and 8YSZ, the DLC consists of the bond coat, the buffer layer with 8YSZ (204 C-NS), and the top coat with 50:50 volume ratio, and the TLC consists of the bond coat, the two buffer layers with 8YSZ (204 C-NS) and with 50:50 volume ratio in LZO and 8YSZ, and the top coat with 50:50 volume ratio. A reference sample was designed using 8YSZ feedstock powders to compare with LZO-based TBCs. Furthermore, the top coat of the reference sample was deposited on the bond coat by using METCO 204C-NS (particle size of 45–125 μm; Sulzer Metco Holding AG) with an APS method. The feedstock of the bond coat for the reference sample was AMDRY 997 (nominal composition of Ni–*22Co*-22Cr–10Al–1.0Y in wt.% and particle size of 56–106 μm; Sulzer Metco Holding AG), and the bond

ACCEPTED MANUSCRIPT

coat was prepared by using a vacuum plasma spray (VPS) process. The thicknesses of the *top and bond coats* were designed as 600 μm and 150μm, respectively. The schematic diagrams of the structural designs *and its cross-sectional microstructures of as-prepared samples* are shown in Fig. 2*, showing the designed and as-prepared microstructures, respectively.*

2.2. TGMF test

The delamination and facture behaviors of TBCs in a combined thermal and mechanical stress environment, particularly for a turbine blade with a specific amount of the mechanical and thermal stresses, were investigated through TGMF tests. The apparatus, schematic diagram, and test condition of the TGMF test are shown *in Fig. 3(A), (B), and (C), respectively.* A uniaxial tensile load (δ_a) of 60 MPa was applied *to a sample with a rate of 1.5 mm/min and strain was controlled with a mechanical strain range of 0.2%*. The applied stress δ_a is defined as $\delta_a = P_a/S_0$, where S_0 is the entire cross-sectional area of the coated sample ($S_0 = w\ (h_{TBC} + h_{BC} + h_S)$), and h_{TBC} = 430 μm, h_{BC} = 150 μm, and $h_S \approx 5.5$ mm are the thicknesses of the top coat, bond coat, and substrate, respectively. TGMF tests were performed for 1000 cycles at a surface temperature of 1100 °C for a dwell time of 10 min, using liquefied petroleum gas, and then the sample was cooled at room temperature for 10 min in each cycle. *The surface temperature of sample at the center and edge regions of flame was different due to the localized flame. Therefore the temperatures at the center and edge were measured by a R-type thermal couple and Infrared-temperature measurement device (Wavelength: 3.9 μm, CTlaser MT, Optris, Germany), respectively.* The criteria that were adopted for failure in the TGMF tests were more than 50% spalling

ACCEPTED MANUSCRIPT

of the region, or cracking in the top coat and/or at the interface.

2.3. Characteristics

For microstructure analysis before and after TGMF testing, the samples were divided into three portions due to the difference in thermal fatigue phenomenon. In this investigation, the sectional views of chosen portions are perpendicular and parallel to the tensile loads applied to the samples. The selected portions of samples were preprocessed to observe the cross-sectional microstructure before and after the TGMF tests. The samples were cold-mounted using epoxy resin, polished using silicon carbide paper and then final polished using 3 μm and 1 μm diamond pastes. The cross-sectional microstructures of the TBC samples were observed using a scanning electron microscope (SEM, Model JSM-5610; JEOL, Tokyo, Japan) in backscattered electron image mode. Delamination at the interface between the buffer layer and *top coat*, and the effect of tensile load on the samples in the thermal environment were observed through these microstructures.

3. Results and discussion

3.1 Characterization of *as*-prepared samples

VPS *process was* used to prepare the bond coat of sample A in the reference sample, *showing a denser microstructure and lower oxide contents than others prepared by APS process [14]*. All of the samples showed an irregular surface roughness at the interface between coating layers and a sound condition without obvious cracks, thermally grown oxide layers, and delamination at the interfaces, *as shown in Fig. 2*. The SLC (sample B), *DLC (sample C), and TLC TBCs (sample D)* were prepared by using the blended feedstock

ACCEPTED MANUSCRIPT

powders for top coats, which were prepared with different volume ratios of 50:50 and 25:75 of LZO and YSZ, respectively. The topcoat was applied by flame in the TGMF test (brown color), as shown in Fig. 1(B). Cross-sectional microstructures of as-prepared TBCs are shown in Fig. 4. The topcoat microstructures showed typical microstructures deposited by the APS method such as splat boundaries, parallel cracks, pores, and unmelted powders *[15]*. The first buffer layer of samples C and D with porous YSZ, and the second buffer layer *of sample D* with blended feedstock (volume ratio 25:75 of LAO and YSZ), were deposited with a thickness of 110 μm and 52 μm, respectively, and the three different ceramic layers could be distinguished precisely. The total thicknesses of the topcoat with first and second buffer layers and bond coat were deposited to approximately 556 μm and 97 μm, respectively.

The effects of the thickness differences were not considered in this investigation because the implication was negligible on thermal durability according to previous studies, although a thick coating may cause thermal and residual stresses *[16,17]*. *The top and bond coats* of sample A were prepared using the APS and VPS processes, respectively.

3.2 Fracture behavior analysis in TGMF test

TGMF testing technique was first developed in late 1990's [18,19]. In these designs, the samples were in cylindrical shape. Mechanical loading was imposed on the sample by a servo hydraulic testing machine. For simultaneous heating around the sample, the radiation of multiple quartz lamps was focused onto the sample by using elliptical mirrors. A temperature gradient was generated from the inner cooling of the sample by controlled air flow. In this study, a flat sample geometry shown in Fig. 1 was employed. This simplifies the

ACCEPTED MANUSCRIPT

setup of experiment and also sample preparation. The photographs at the surfaces and sides of all samples after the TGMF tests at 1100 °C and tensile loads of 60 MPa for 1000 cycles are shown in *Fig. 4, and the lifetime performance of TBCs in the TGMF tests are indicated in Table 1. In this study, only one sample was tested at each condition, due to limited number of samples. In the future work, we will test multiple (> 3) samples to find out the mean values and variations of the results. For the TLC TBC, the test was stopped at 1000 cycle due to experimental set up. In the future, we will run the test until the sample fails to find out true cycle numbers of failure.* After the TGMF test, cracks resulted on the surfaces and interfaces of the samples, except in sample D. These cracks were observed after 850 cycles, 910 cycles, and 960 cycles in samples A (reference sample), B, and C, respectively. Even though it was checked with a visual inspection, sample D showed a sound condition after 1000 cycles. *The result is consistent with the previous study [20], in which the lifetimes of TBCs with APS bond coats were similar to or superior to those of TBCs with VPS bond coats. The results suggest that APS bond coats, which are more cost-effective, may be competitive with VPS bond coats for certain TBC applications. In terms of bond coat composition, the CTEs of NiCrAlY (about* $1\times10^{-6}\ K^{-1}$*) are lower than those NiCoCrAlY in the same temperature range 25 to 1200 °C [20], suggesting higher residual stress should be generated between the bond and top coats when the bond coat with NiCoCrAlY composition is used in the LZO composite coatings.*

The cross-sectional microstructure of samples after the TGMF tests is shown in *Fig. 5, including schematic diagram for observing microstructures with the flame position and the direction of applied load. Figure 5 is the microstructures observed at the center of the flame in the parallel direction of the applied load.* In the reference sample *(Fig. 5(A)),* the vertical cracks, which are perpendicular to the direction of tension load, and the parallel cracks at the interface between the bond and top coats, were generated. SLC and DLC TBCs *(Fig. 5(B)*

ACCEPTED MANUSCRIPT

and (C)) generated the long parallel *cracks* within the top coat near the interface and the significant vertical *cracks* at the center. Even though the lifetime performances of samples A to C are not significantly different, the fracture behavior or status of the single-layer TBCs (samples A and B) was worse than that of *the DLC TBC sample (sample C). However, the TLC sample (sample D) shows a sound condition after the TGMF test with a few narrow vertical cracks. The composite TBCs with the buffer layer (samples C and D) were delaminated and/or cracked at the interface between the buffer layer and the top coat, not close to the bond coat.* Cross-sectional microstructure observations can verify that the vertical crack is preferentially created and then the parallel crack is propagated in the TGMF environment.

The fracture behavior can be well defined in the highly magnified microstructures. Therefore, comparisons of highly magnified microstructures in the parallel direction are shown in Figs 6 and 7, which show portions of tested samples at the center and the edge of the flame, respectively. The highly magnified cross-sectional microstructures for the parallel direction of the applied load are shown in *Fig. 6.* The SLC TBCs showed similar crack propagation behavior in parallel cracking, which is usually created within 150 μm from the interface, while the parallel crack was formed between the buffer layer and the top coat, or near the interface in the DLC TBC, with a vertical crack passing the buffer layer *(Fig. 5 (C)).* However, sample D displayed more remarkable thermal durability in TGMF tests, with narrow vertical cracks near the surface and an otherwise sound condition. In the comparison of LZO-based TBCs, the CTE mismatch between the bond coat and the composite top coat was reduced by introducing the buffer layer, and the mismatch could be more reduced with relatively graded composition *[21]*. It may be assumed that small cracks that propagated vertically in the regions of initial tensile stress will grow into larger

ACCEPTED MANUSCRIPT

cracks near the top coat boundary. The parallel cracks at the interface between the buffer layer and the top coat, and/or between *the bond and top coats,* indicated that the thermal and residual stresses were induced as a result of the CTE mismatch *[22]*. *The expected CTE values of the composite layers can be estimated from using the mixing rule. For example, if approximating the CTE values for LZO and YSZ are 9 ×10^{-6} K^{-1}, and 11×10^{-6} K^{-1}, respectively, the CTE values of 75:25 and 50:50 vol. ratio of mixed YSZ-LZO would be 10.5×10^{-6} K^{-1} and 10×10^{-6} K^{-1}, respectively. The key idea to improve the multi-layer coating's durability is to produce a graded transition in their CTE values and mechanical properties.* Therefore, the buffer layer could reduce the CTE mismatch between the bond coat and topcoat effectively, and the TLC TBCs samples showed superior thermal durability and fracture resistance.

The highly magnified cross-sectional microstructures for the parallel direction of the applied load are shown in Fig. 7, including schematic diagram for observing microstructures with the flame position and the direction of applied load. Obviously, the LZO-based TBC samples showed a notable difference in mechanical properties when the samples were at a lower temperature, probably at 900 °C. The LZO-based TBC samples, except the TLC sample, showed more vertical cracks than sample A because the mechanical properties of the top coat were reduced by adding LZO to the top coat. However, the TLC sample showed a sound condition because of reduced CTE mismatch by introducing the second buffer layer. Sample A and the TLC samples (sample D) were verified with better mechanical properties than other LZO-based samples. Both the mechanical properties of the top coat material and the design of the TBC system are important factors to enhance the lifetime performance of the TBC system at a low

ACCEPTED MANUSCRIPT

temperature. Furthermore, in samples B and C, vertical cracks were easily propagated to the interface between the porous YSZ buffer layer and the LZO layer, from which the parallel cracks were then generated. The CTE mismatch between the LZO layer and the YSZ buffer layer caused the crack generation in the low temperature thermomechanical environment.

In Fig. 8, the cross-sectional microstructures of the portions are perpendicular to the tensile load in the TGMF test. Cracks were not found in the highly magnified microstructure in the parallel direction *in Fig. 9.* The crack initiation and propagation behaviors were affected by the direction, showing sound condition in the vertical direction to the applied load. This phenomenon could surmise that the perpendicular cracks to the tensile load constituted the primary fracture behavior in the TGMF test. The fracture behavior was initiated on the surface of the ceramic coating, propagated towards to the interface between the top coat/buffer layer and bond coat, and transverse cracks were deflected at that interface *[23]*. The interface cracks within the top coat layer, propagating parallel to that interface, finally resulted in the spallation of the ceramic coating *[24]*. It was expected that transverse cracks in the topcoat layer should deflect at the interface between the ceramic coat and bond coat due to the difference in mechanical properties between metal and ceramic materials *[23]*. The fracture behavior in this investigation compares well with previous work on brittle coatings *[25–28]*.

4. Conclusions

The lifetime performance of LZO-based TBCs was investigated through TGMF tests and the following conclusions were obtained. Multilayered TBCs using composite

ACCEPTED MANUSCRIPT

feedstock powders were well prepared and the buffer layers in *the* DLC and TLC TBCs were 8YSZ and 8YSZ/composite layer with a volume ratio 25:75 of LZO and YSZ, respectively. Thermal durability was improved by microstructure design using composite coating and buffer layers. Among all the samples, the *TLC TBC sample* showed the most outstanding thermal durability in the TGMF tests. The introduced buffer layer improved thermal durability due to the reduced thermal and residual stresses at the interfaces by decreasing CTE mismatch with relatively continuous composition variation. Vertical cracks initiated at the top surface during the TGMF tests and then propagated towards to the interface between the top coat and the buffer layer or between the top and bond coats, followed by transverse cracking. The crack initiation and propagation behaviors were affected by the direction, showing a sound condition in the perpendicular direction to the applied load. This investigation provided an effective way to protect the substrate in LZO-based TBCs system under combined thermal and mechanical environments.

Acknowledgements

This work was supported by "Human Resources Program in Energy Technology" of the Korea Institute of Energy Technology Evaluation and Planning (KETEP), granted financial resource from the Ministry of Trade, Industry & Energy, Republic of Korea (No. 20174030201460) and by Fundamental Research Program of the Korean Institute of Materials Science (KIMS).

ACCEPTED MANUSCRIPT

References

[1] G.W. Goward, Surf. Coat. Technol. 73–79 (1998) *108–109.*

[2] W. Beele, G. Marijnissen, A. van Lieshout, Surf. Coat. Technol. 120–121 (1999) 61.

[3] C. Soares, The Gas Turbine Handbook, R. Dennis, ed., NETL, Morgantown, WV (1998).

[4] R. Vassen, X. Cao, F. Tietz, D. Basu, D. Stöver, J. Am. Ceram. Soc. 2023–2028 (2000) 83(8).

[5] K.W. Schlichting, N.P. Padture, P.G. Klemens, J. Mater. Sci. 3003–3010 (2001) 36(12).

[6] D.P.H. Hasselman, L.F. Johnson, L.D. Bentsen, R. Syed, H.L. Lee, M.V. Swain, J. Am. Ceram. Soc. Bull. 799–806 (1987) 66(5).

[7] X.Q. Cao, R. Vassen, W. Jungen, S. Schwartz, F, Tietz, D. Stöver, J. Am. Ceram. Soc. 2086–2090 (2001) 84(9).

[8] J. Zhang, X.Y. Guo, Y.G. Jung, L. Li, J. Knapp, Surf. Coat. Technol. 18–29 (2017)323.

[9] J. Thornton, A. Majumdar, A. Ohmori, Proce. 14th. Int. Therm. Spray. Con., ASM Int., 1075–1080 (1995).

[10] X.Q. Cao, R. Vassen, *D. Stöver,* J. Eur. Ceram. Soc. 1–10 (2004) 24(1).

[11] X.Q. Cao, R. Vassen, F. Tietz, Stöver, J. Eur. Ceram. Soc. 247-251 (2006) 26(3).

[12] X.Q. Cao, J. Mater. Sci. Technol. 15–35 (2007) 23.

[13] D.W. Song, U.G. Paik, X.Y. Guo, J. Zhang, T.K. Woo, Z. Lu, S.H. Jung, J.H. Lee, Y.G. Jung, Surf. Coat. Technol. 40–49 (2016) 308.

[14] M. Di Ferdinando, A. Fossati, A. Lavacchi, U. Bardi, F. Borgioli, C. Borri, C. Giolli, A. Scrivani, Surf. Coat. Technol. 2499–2503 (2010) 204(15).

[15] N.P. Padture, M. Gell, E.H. Jordan. J. Sci. 280–284 (2002) 296 (5566).

[16] Y. Radin, T. Kontorovich, International Conference on Power Energy System, 175–178 (2012) 13.

ACCEPTED MANUSCRIPT

[17] T.W. Clyne, S.C. Gill, J. Therm. Spray Technol. 401–418 (1996) 5(4).

[18] M. Bartsch, G. Marci, K. Mull, C. Sick, Advan. Engin. Mater. 127–129 (1999) 1.

[19] B. Baufeld, M. Bartsch, M. Heinzelmann, Inter. J. Fatigue 219–225 (2008) 30.

[20] J. A. Haynes, M. K. Ferber, and W. D. Porter, J. Therm. Spray Technol. 38–48 (2000) 9(1).

[21] H. Meng, J.H. Huang, S.H. Chen, *Ceram. Inter.* 2901–2914 (2014) 40(2).

[22] G.C. Chang and W. Pucharoen, Surf. Coat. Technol. 307–325 (1987) 32.

[23] A. Kawasaki and R. Watanabe, J. Engin. Fracture Mech. 1713–1728 (2002) 69(14).

[24] W.G. Mao, C.Y. Dai, L. Yang, Y.C. Zhou, Inter. J. Fracture, 107–120 (2008) 151(2).

[25] L. Qian, S. Zhu, Y. Kagawa, T. Kubo, Surf. Coat. Technol. 178–184 (2003) 2(173).

[26] M. Wen, H.E. Jordan, and M. Gell, Surf. Coat. Technol. 5193-5202 (2006) 200(18).

[27] Y.H. Sohn, J.H. Kim, E.H. Jordan, M. Gell, Surf. Coat. Technol. 70–78 (2001) 146.

[28] M.S. Hu, and A.G. Evans. Acta Metallurgica. 917‒925 (1989) 3(37).

ACCEPTED MANUSCRIPT

ACCEPTED MANUSCRIPT

Table captions

Table 1. Lifetime performance of TBCs in TGMF tests

Figure captions

Fig. 1. *Schematic diagram and real sample tested in this study:* (A) Shape and dimensions of the LZO-based TBCs samples in TGMF test. (B) Surface and side photographs of as-prepared LZO-based TBCs samples.

Fig. 2.*Schematic diagram and cross-sectional microstructure designed and prepared in this study. Each number indicates the designed and as-prepared microstructures, respectively.*

Fig. 3. Apparatus and schematic diagram of TGMF test: (A) photographs of apparatus, (B) schematic diagram, and (C) test conditions.

Fig. 4. Surface and side photographs after TGMF test. Each number indicates the surface and side photograph, respectively.

Fig. 5. Microstructures *at the center of the flame in the parallel direction of the applied load and schematic diagram for observing microstructures with the flame position and the direction of applied load.*

Fig. 6. Highly magnified microstructures *at the center of the flame in the parallel direction of the applied load*.

Fig. 7. Highly magnified microstructures *at the edge of the flame in the parallel direction of the applied load*.

Fig. 8. Microstructures *at the center of the flame in the perpendicular direction of the applied load and schematic diagram for observing microstructures with the flame position and the direction of applied load.*

Fig. 9. Highly magnified microstructures *at the center of the flame in the perpendicular*

ACCEPTED MANUSCRIPT

direction of the applied load.

ACCEPTED MANUSCRIPT

ACCEPTED MANUSCRIPT

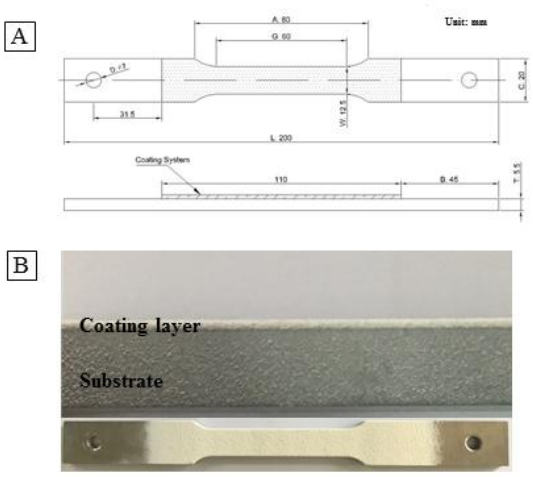

Fig. 1.

ACCEP

ACCEPTED MANUSCRIPT

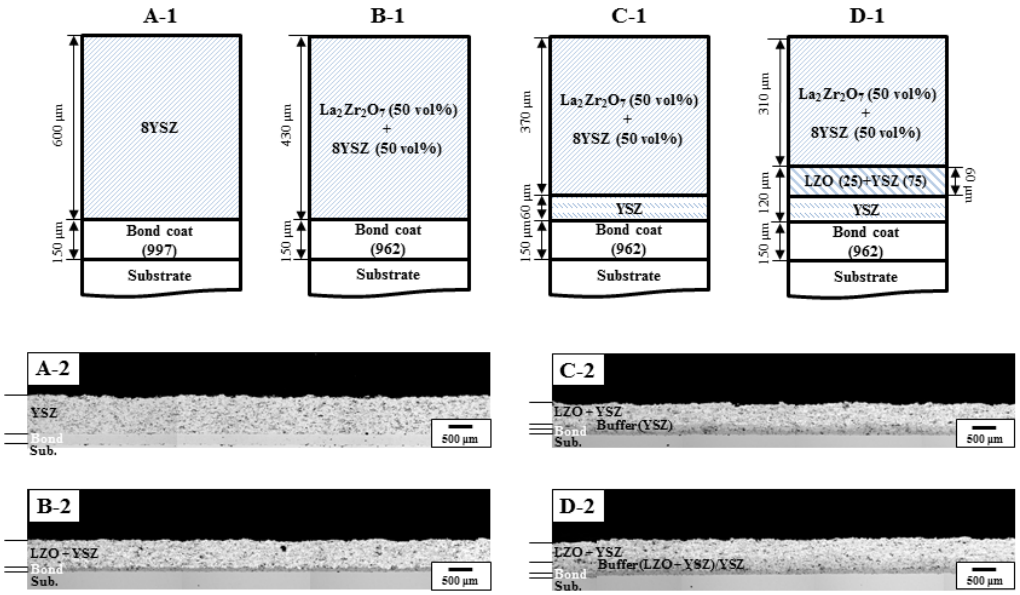

Fig. 2.

ACCEPTED

ACCEPTED MANUSCRIPT

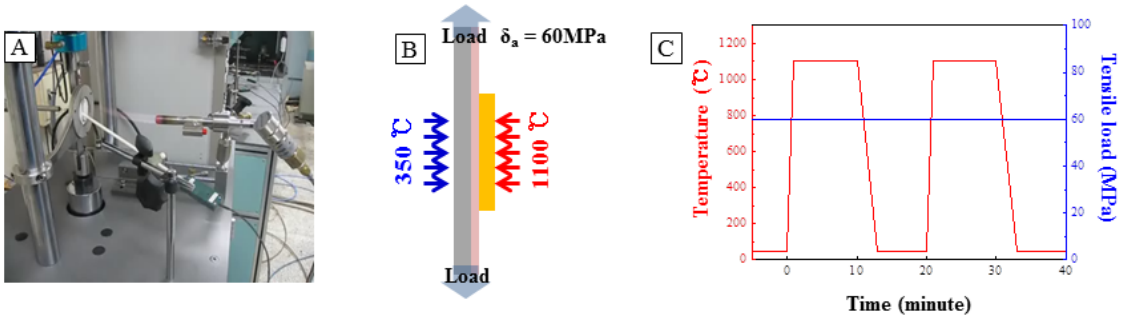

Fig. 3.

ACCEPTED

ACCEPTED MANUSCRIPT

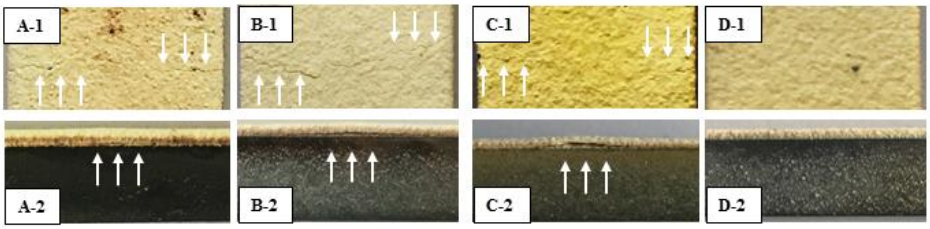

Fig. 4.

ACCE

ACCEPTED MANUSCRIPT

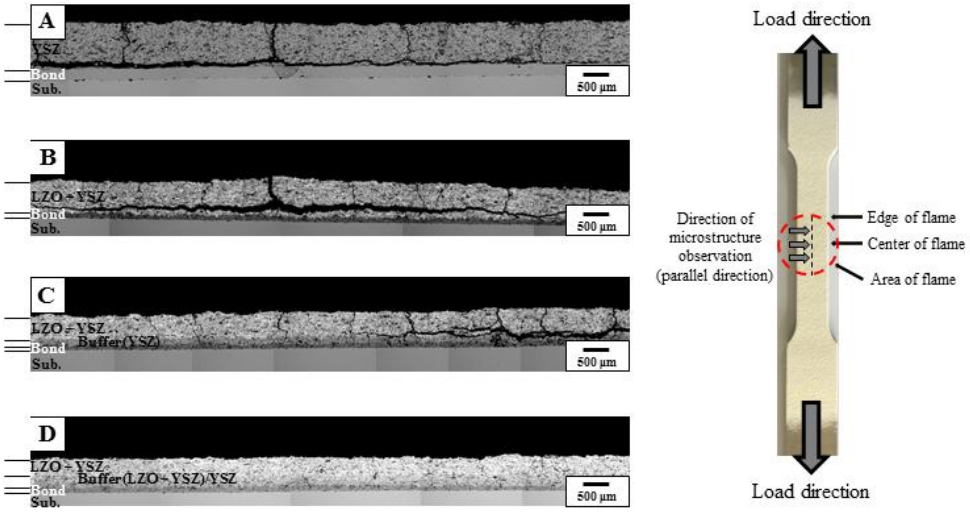

Fig. 5.

ACCEP

ACCEPTED MANUSCRIPT

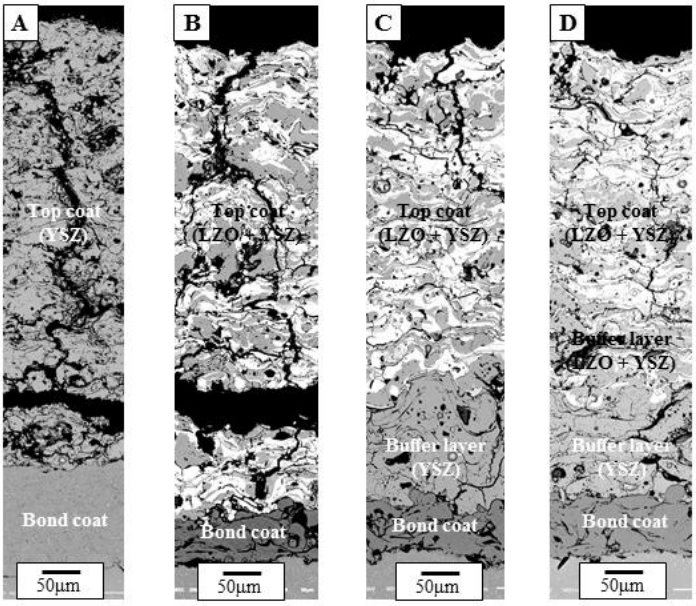

Fig. 6.

ACCEPTED

ACCEPTED MANUSCRIPT

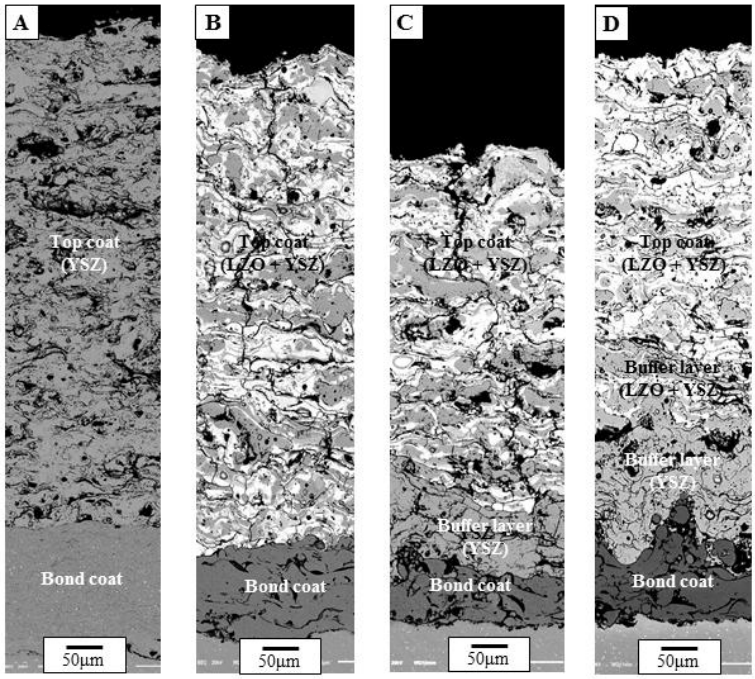

Fig. 7.

ACCEPTED

ACCEPTED MANUSCRIPT

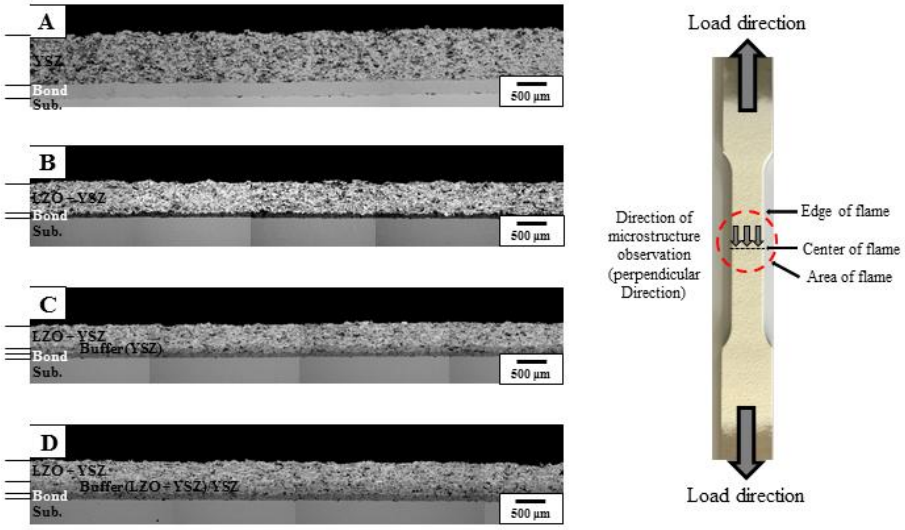

Fig. 8.

ACCEP

ACCEPTED MANUSCRIPT

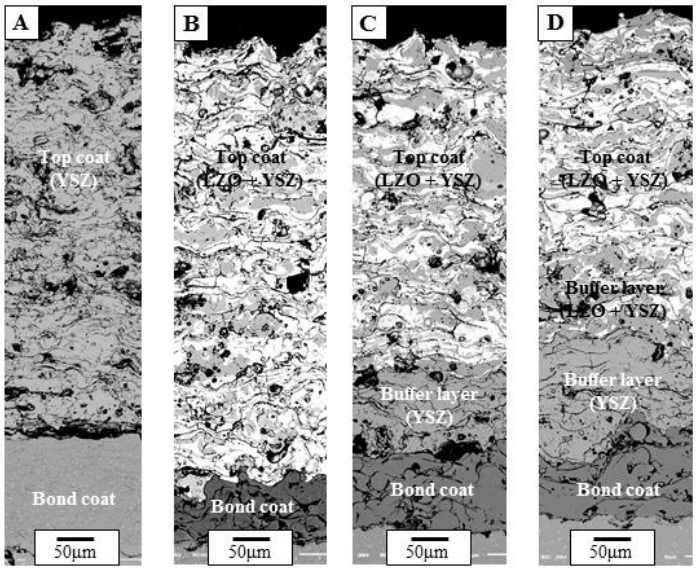

Fig. 9.

ACCEP

ACCEPTED MANUSCRIPT

Sample	Bond coat	Buffer layer	Top coat	TGMF test at 1100°C	Remarks
A	AMDRY 997	None	8YSZ	1000 cycles	Cracked at 850 cycles
B	AMDRY 962	None	LZO (50 vol%) + 8YSZ (50 vol%)		Cracked at 910 cycles
C		8YSZ			Cracked at 960 cycles
D		LZO (25 vol%) + YSZ (75 vol%) / 8YSZ			Sound condition

Table 1

ACCEPTED MANUSCRIPT

ACCEPTED MANUSCRIPT

Research Highlights:

- Multilayered LZO-based TBCs were well prepared using composite powders.
- The lifetime performance of LZO-based TBCs was investigated through TGMF test.
- TBC with triple-layered top coat showed the most outstanding thermal durability.
- Crack initiation and its growth behavior were affected by the direction of applied load.

ACCEPTED MANUSCRIPT